Astron. Astrophys. 356, 747–756 (2000)

ASTRONOMY AND ASTROPHYSICS

Temporary orbital capture of ejecta from comets and asteroids: Application to the Deep Impact experiment

D.J. Scheeres[1] **and F. Marzari**[2]

[1] The University of Michigan, Department of Aerospace Engineering, Ann Arbor, Michigan 48109–2140, USA (scheeres@umich.edu)
[2] University of Padova, Department of Physics, 35131 Padova, Italy (marzari@pd.infn.it)

Received 31 December 1999 / Accepted 20 January 2000

Abstract. The trajectories of dust particles ejected from the surface of a comet or asteroid after a cratering impact are influenced by the interplay of solar radiation pressure, solar tide, cometary outgassing (for comets) and the body's irregular gravity field. In this paper we evaluate the ability of these forces to cause ejecta to become captured in temporary orbits about the parent body. We concentrate on the effect of solar radiation pressure and compute conditions in which particles can be caught in temporary orbits. The first order effects of the solar tide, comet outgassing, and body gravity field are also discussed. Our analysis uses the approximation introduced by Richter & Keller (1995) which gives an analytical solution of the averaged equations of motion under the assumption that the radiation pressure is the dominant perturbative force. We validate that this approximation works properly under the special orbital conditions which ejecta have – characterized by high eccentricities and large semimajor axes. As a specific example, we use the theory to analyze the trapping of particles following the Deep Impact experiment, which will send a man-made impactor into the comet Tempel 1. The theory can be extended to other small solar system bodies as well.

Key words: solar system: general – comets: general – minor planets, asteroids

1. Introduction

In recent years the scientific community has focused on the study of small solar system bodies, due to the information that they contain about the formation and evolution of the solar system. After an initial phase characterized by flybys to comets and asteroids by major planetary missions (Galileo, CASSINI) or by dedicated missions (GIOTTO, Sakigate & Suisei, Vega1 & 2), a series of rendezvous-missions are being planned to allow extended and detailed exploration of these bodies. NEAR, ROSETTA and MUSES-C will orbit for several months around a comet or asteroid to study in detail their morphology, physical properties and evolution with time. When a spacecraft is in close proximity to such a small body it is exposed to the risk of being hit by particles trapped in long-lifetime orbits around the body. Small particles (on the order of millimeters to centimeters) can be injected into temporary capture orbits after cratering impacts or intense cometary outgassing, since in this size range the solar radiation pressure significantly influences the dynamical evolution of the particles and may transition them into orbits with lifetimes on the order of hundreds of days or longer.

Small energy cratering events, capable of lofting a significant amount of ejecta off of a small body, occur frequently on asteroids and could also occur on comets that spend a significant amount of their orbit in the main belt, like comet Wirtanen, the target of the ROSETTA mission. Outgassing phenomena on a comet surface during a perihelion passage can also eject large amounts of dust from the surface that can be trapped in temporary orbits, forming a cloud surrounding the nucleus of the comet.

An interesting experiment that will simulate an impact event on the surface of a comet is represented by the Deep Impact experiment (Meech et al. 1999). The Deep Impact (DI) Discovery mission is designed to release a 500 kg impactor that will collide with comet Tempel 1 at a relative speed of about 10 km/s. This experiment, intended to probe the material strength of the comet and to reveal the inner composition of the nucleus, mimics a natural cratering event on the surface of the comet. Ejecta from such a cratering event may re-impact on the surface of the nucleus, escape on hyperbolic orbits, or be trapped in temporary orbits around the nucleus. Images taken after the impact may allow initial orbit parameters of crater fragments to be determined, leading to a model of the subsequent dynamical evolution of the ejecta blankets.

Numerical calculations of simulated ejecta blankets from impacts on the asteroid Ida have been performed by Geissler et al. (1996) via direct numerical integration of the equations of motion. However, their study is limited to the effects of nonsphericity and rotation of the asteroid on the trajectory of particles launched from an impact site. In this paper we consider ejecta with diameters on the order of centimeters and smaller. In this size range the solar radiation pressure force is, by far, the leading perturbing force. Richter & Keller (1995) re-derived an analytic closed form solution (denoted as RPA) to the equations of motion for a dust particle moving around a spherical body (in an eccentric orbit around the sun) and perturbed by the radiation pressure (see Mignard & Hénon 1984 for an earlier discussion of this solution). This solution predicts the evolution of the orbital elements of a dust particle and can be used to estimate the

time spent orbiting around the comet before re-impact on the comet surface occurs.

Since we are dealing with dust ejected on nearly rectilinear orbits with very large eccentricity, we first tested the RPA solution against the numerical solution in this range of eccentricity. Once we define the limits of applicability for the RPA approximation, we analytically derive the conditions for dust particles to become trapped in orbit about the comet (or asteroid) and the lifetime of these orbits as a function of ejection speed and particle size. We show that the lifetime of the dust particles depends strongly on their size and on the ejection velocity. The maximum particle size which can be trapped into orbit around the comet can be computed as a function of ejection site, particle size, and ejection speed.

One limitation of our approach for computing ejecta orbits is that the RPA solution does not include all the possible perturbations to the dynamics of a dust particle. When close to the comet surface, the particle orbit may deviate significantly from the RPA solution due to gravity and outgassing, while far from the comet the solar tide may strongly perturb the solution. Thus, we also discuss the possible effects of these perturbations to first order. Future analysis of this problem will improve the characterization of these effects and include them into one general model.

Since we cannot analyse all the possible configurations of cratering events on asteroids or comets, we concentrate our study on the DI experiment. Both the analytical predictions and numerical simulations are assumed to have similar initial conditions to the DI experiment.

In Sect. 2 we discuss the basic mechanics of how the solar radiation pressure (SRP) force can cause particles to become captured. In Sect. 3 we discuss the effect of the averaging approximation and other perturbations on these mechanics. In Sect. 4 we apply our model to the Deep Impact crater experiment to compute global conditions for particle trapping. Finally, in Sect. 5 we discuss the results and give conclusions.

2. Mechanics of temporary orbital capture

2.1. Orbit mechanics of ejected particles

We assume that a particle is ejected from the surface of a comet at an arbitrary latitude and longitude (δ and α respectively), specified in the fixed comet-sun coordinate frame: x-axis measured positive pointing away from the sun, z-axis positive along the comet's orbit angular momentum about the sun, and y-axis positive along the direction of comet travel. The semi-major axis of the ejected particle is a free parameter and is assumed to be positive, corresponding to a bound orbit, and can be directly related to the ejection speed of the particle.

The initial position vector of the particle can then be specified as:

$$\mathbf{r} = r\hat{\mathbf{r}} \tag{1}$$

$$\hat{\mathbf{r}} = \cos\alpha\cos\delta\hat{\mathbf{x}} + \sin\alpha\cos\delta\hat{\mathbf{y}} + \sin\delta\hat{\mathbf{z}} \tag{2}$$

in terms of the latitude and longitude of the ejection site. The initial velocity vector is determined by two additional angles: the angle γ giving the inclination of the velocity respect to the vertical, and the angle β giving the orientation of the velocity vector tangent to the comet surface. Without any additional perturbations these orbits will fall back onto the comet surface as their initial periapsis lies beneath the surface.

We use these initial conditions for ejecta particles with an analytical approach developed by Mignard & Hénon (1984) and Richter & Keller (1995) for averaged particle motion in the presence of solar radiation pressure. This formulation allows us to explicitly compute the orbital elements of a particle at any future date. Due to the SRP force, orbits that initially have periapsis under the surface of the comet can transition into orbits with periapsis radius above the comet surface – allowing the particles to survive for more than one orbit about the comet. Since these solutions are periodic, the particle will eventually re-impact on the comet surface, but the time to re-impact may be many months.

Richter & Keller (1995) develop a very simple and concise form for the general solution of particle evolution under averaged SRP force. This solution was previously investigated in a slightly different form by Mignard & Hénon (1984). These general solutions incorporate the effect of the comet moving on an elliptic orbit about the sun – accommodating both the change in SRP force magnitude and direction. The major drawback is that this solution ignores the perturbations that the particle feels due to the comet gravity field, comet outgassing and solar tide. The first order effect of these perturbations are discussed later. The solution also does not provide any prediction of when the particle lies far enough from the central body to be stripped away by the combination of solar tide and SRP forces. Approximate limits for this limiting semi-major axis are available, however (Hamilton & Burns 1992).

There is only one free parameter that needs to be specified for the solution, combining the comet semi-major axis and eccentricity, the strength of the SRP force, the radius of the ejected particles, the mass of the sun, the mass of the comet and the particle semi-major axis. This parameter is invariant with respect to the comet distance from the sun. Following Mignard & Hénon (1984) we express this parameter as an angle ψ:

$$\tan\psi = \frac{3G_1}{2B}\sqrt{\frac{a}{P\mu\mu_s}} \tag{3}$$

$$\sim 0.75\frac{\sqrt{a}}{r_c} \tag{4}$$

where $G_1 = 1\times10^8$ (kg km^3/s^2/m^2) is the SRP strength parameter, B is the mass to projected area ratio of a sphere of radius r_c, a is the particle semi-major axis about the comet, P is the comet orbit parameter about the sun, μ is the comet mass parameter, and μ_s is the sun's mass parameter. Formula 4 gives this parameter for particles ejected from Tempel 1 with a semi-major axis a (in kilometers) and a particle radius r_c (in centimeters), see Table 1. The angle ψ parameterizes the relative strength of the SRP, for a small dust particle the angle approaches $\pi/2$ while for a large particle the angle approaches 0.

Table 1. Assumed parameters for comet Tempel 1

Parameter	Symbol	Assumed Value
Comet Perihelion Radius	q	1.506 AU
Comet Eccentricity	e	0.5175
Comet mean radius	R_o	3 km
Comet mean density	ρ	1 g/cm^3
Comet mass parameter	μ	7.55×10^{-6} km^3/s^2

The form of the solution given by Richter & Keller (1995) describes the evolution of the orbit angular momentum vector and apocenter vector as a function of comet true anomaly ν about the sun. The averaged solution is periodic in true anomaly with period $2\pi \cos\psi$, thus the averaged solutions we find will repeat themselves after the comet has moved through this angle. Thus when the comet is in an elliptic orbit the period of motion is shorter around periapsis than it is around apoapsis. We note that for stronger perturbations (i.e., for smaller particles) the period of these averaged solutions will decrease. In the limit for a large particle ($\psi \to 0$) we see that the period of the averaged motion approaches the comet orbit period about the sun.

To compute the solution we derive the initial angular momentum and apocenter vectors from the particle position and velocity. Then we compute the values of the angular momentum and apocenter vector as functions of time using the theory. We note that the semi-major axis of each particle orbit is assumed to be constant on average (Mignard & Hénon 1984). We then have an explicit prediction for the evolution of the particle orbit as a function of the SRP parameter ψ and its ejection conditions.

2.2. Capture and escape conditions

Using the analytical solution we generate conditions for a given particle to not re-impact after one orbit period, and hence be "lofted" into a longer term orbit about the comet. First, we choose an impact site (angles δ and α), an initial semi-major axis (a) for the orbit, and an initial pair of angles γ and β for the ejection direction. Choosing the semi-major axis is equivalent to choosing the ejection speed V_c at the surface of the comet:

$$V_c^2 \sim 2\mu \left[\frac{1}{R_o} - \frac{1}{2a} \right] \tag{5}$$

where R_o is the mean radius of the comet.

Given the orbit semi-major axis (or the ejection speed on the surface) we have defined the orbit period for the particle, and can then derive a constraint on the orbit eccentricity after one period so that the particle will not re-impact on the comet surface. If we specify the orbit period as $T = 2\pi a^{3/2}/\sqrt{\mu}$, and the eccentricity after one orbit period as $e(T)$, then the constraint to not impact on the comet surface after the initial orbit is:

$$e(T) < 1 - \frac{R_o}{a} \tag{6}$$

which is derived by making the orbit periapsis lie above the surface of the comet.

If the radius of the ejected particle, r_c, is specified we can compute the SRP parameter ψ and explicitly compute $e(T)$. Note that to perform this computation the change in comet true anomaly over a time period T must be computed, for which we must solve Kepler's equation for the comet's motion about the sun. Once a particle is captured into orbit it can complete a number of orbits before re–impacting on the nucleus. Since eccentricity varies significantly over one particle orbit period, at any periapsis passage it will have different values. If the eccentricity satisfies Eq. 6 at periapsis the particle will perform another full orbit, and so on. The period of the eccentricity evolution depends on the size of the particle, larger grains will have longer eccentricity cycles. Since re–impact on the surface will occur when the eccentricity returns to its starting value at the end of the cycle, larger particles may have longer capture periods. This is mitigated, however, by having a slower change in eccentricity, meaning that there is a longer "window" of opportunity for impact to occur whenever eccentricity returns to its initial value.

With this analytical approach, we can easily compute, for a given particle radius and ejection geometry, the interval of ejection velocities for temporary orbital trapping and their relative lifetimes. There is an upper bound to the ejection velocities against escape, which is generally less than escape speed proper. This is evaluated accounting for the effect of solar tide and solar radiation pressure with the formula:

$$a < \frac{d}{4}\sqrt{\frac{\mu B}{G_1}} \tag{7}$$

(Scheeres & Marzari submitted) where a is the semimajor axis (km), and d is the comet–sun distance.

2.3. Averaged solution for a special case

To provide a simple, yet concrete, example of the solutions we use for the evolution of the particles under the SRP force we present the closed-form formula for the angular momentum and apocenter vector of a particle initially ejected from the comet on a rectilinear orbit (i.e., with $\gamma = 0$ and $e = 1$). The form of the solution given by Richter & Keller (1995) describes the evolution of the orbit angular momentum $\mathbf{L}$ and apocenter vector $\mathbf{e}$ (where $|\mathbf{e}| = e$) as a function of comet true anomaly ν about the sun. Instead of the comet true anomaly, we use a scaled parameter $H = \nu/\cos\psi$. The solution is then periodic in H with period 2π, thus the averaged solutions we find will repeat themselves after the comet has moved through a true anomaly of $2\pi\cos\psi$. Evaluating the constants for our special initial conditions:

$$\mathbf{L}(0) = 0 \tag{8}$$

$$\mathbf{e} = \hat{\mathbf{r}} \tag{9}$$

results in the closed form solution:

$$L_x = \sin\psi\cos\psi\sin\delta\,(1-\cos H) \tag{10}$$

$$L_y = \sin\psi\sin\delta\sin H \tag{11}$$

$$L_z = \sin\psi\cos\psi\cos\alpha\cos\delta\,(1-\cos H)$$

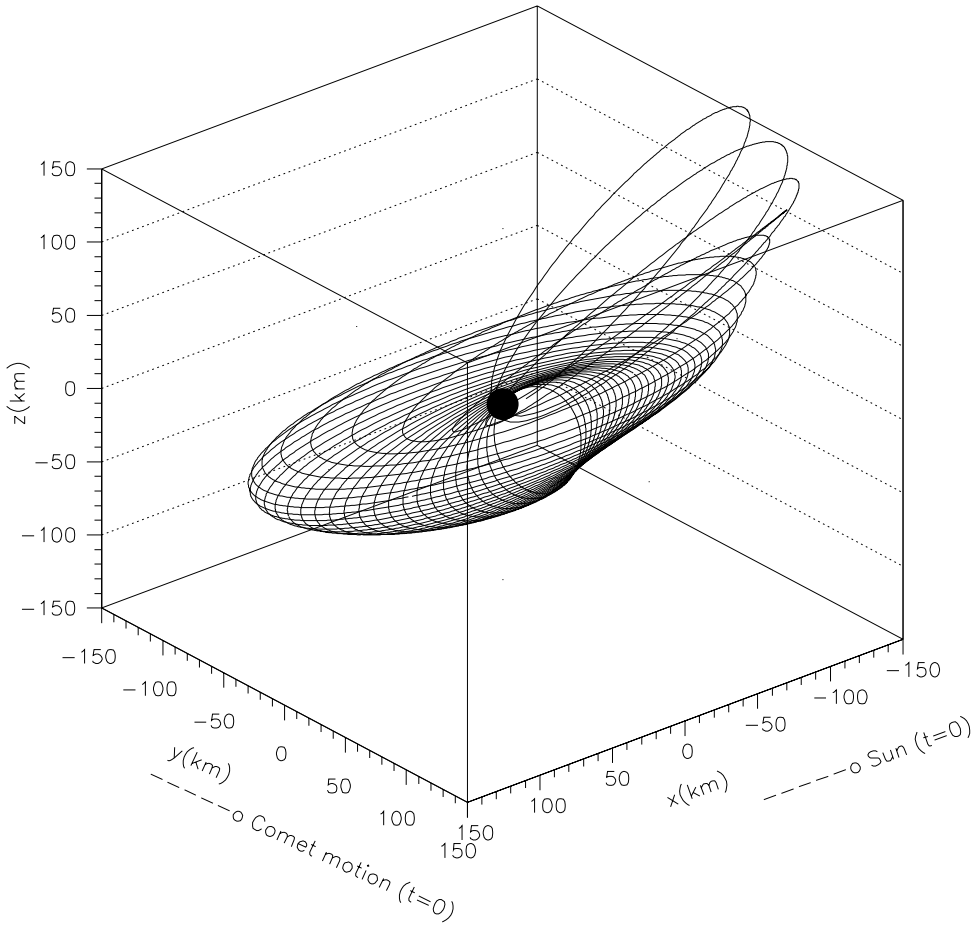

Fig. 1. Single particle orbit trajectory, trapped around the comet for 3.8 years; 5 cm particle ejected with a speed of 2.23 m/s.

$$- \sin\psi \sin\alpha \cos\delta \sin H \tag{12}$$

$$e_x = \cos\alpha \cos\delta \left(\sin^2\psi + \cos^2\psi \cos H\right) + \cos\psi \sin\alpha \cos\delta \sin H \tag{13}$$

$$e_y = \sin\alpha \cos\delta \cos H - \cos\psi \cos\alpha \cos\delta \sin H \tag{14}$$

$$e_z = \sin\delta \left(\cos^2\psi + \sin^2\psi \cos H\right). \tag{15}$$

We then have an explicit prediction for the evolution of the particle orbit as a function of the SRP parameter ψ and the ejection latitude and longitude. A particular solution for an ejected particle at Tempel 1 is shown in Fig. 1.

3. Corrections to capture and lifetime computations for RPA

The above analysis was carried out making averaging and modeling assumptions which may be violated in the comet or asteroid environment. In this section we consider the possible effect these assumptions have on the basic capture mechanics described above. We first focus on the effect of the averaging assumption, then briefly consider the effects of the solar tide, the non-spherical gravity field, and comet outgassing.

3.1. Comparison between RPA and numerical integration

RPA is an approximate theory based on averaging and thus may have a limited range of validity (Richter & Keller 1995). In cratering events we are dealing with highly eccentric orbits, while the numerical tests performed by Richter and Keller were limited to eccentricities lower than 0.8. For the DI experiment, in particular, the impact on the surface of the comet occurs at the perihelium of the comet, where the true anomaly of the comet changes very rapidly. Before using RPA to study the range of ejection velocities for capture and the lifetimes of temporary orbits, we first tested the reliability of RPA by comparing its predictions with the results of direct numerical integration of dust particle orbits. For our system we used the Tempel 1 definitions given in Table 1.

The numerical integration of the orbits have been performed with the RADAU numerical integrator (Everhart 1985). A fixed inertial reference frame, with x-axis measured positive pointing away from the sun, z-axis positive along the comet's orbit angular momentum about the sun, and y-axis positive along the direction of comet travel have been adopted. In comparing the numerical results with the RPA predictions, we have taken into account that the reference system used in RPA is pulsating with the comet orbital motion. The appropriate trasformations were applied to the initial conditions to account for the difference in the reference systems.

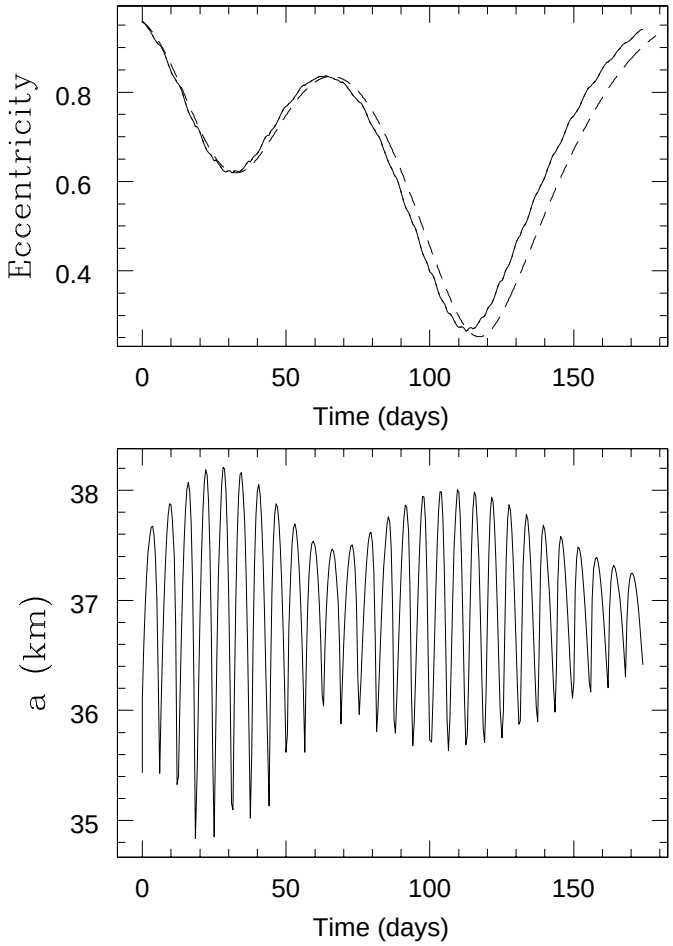

Fig. 2. Eccentricity and semimajor axis of a 1 cm dust grain ejected from the surface of comet Tempel 1 after the DI experiment. The continuous line is the evolution computed with numerical integration while the dotted line is the prediction of the RPA theory. The solar tide is responsible for the small oscillations of the semimajor axis. RPA assumes a constant orbital semimajor axis, on average.

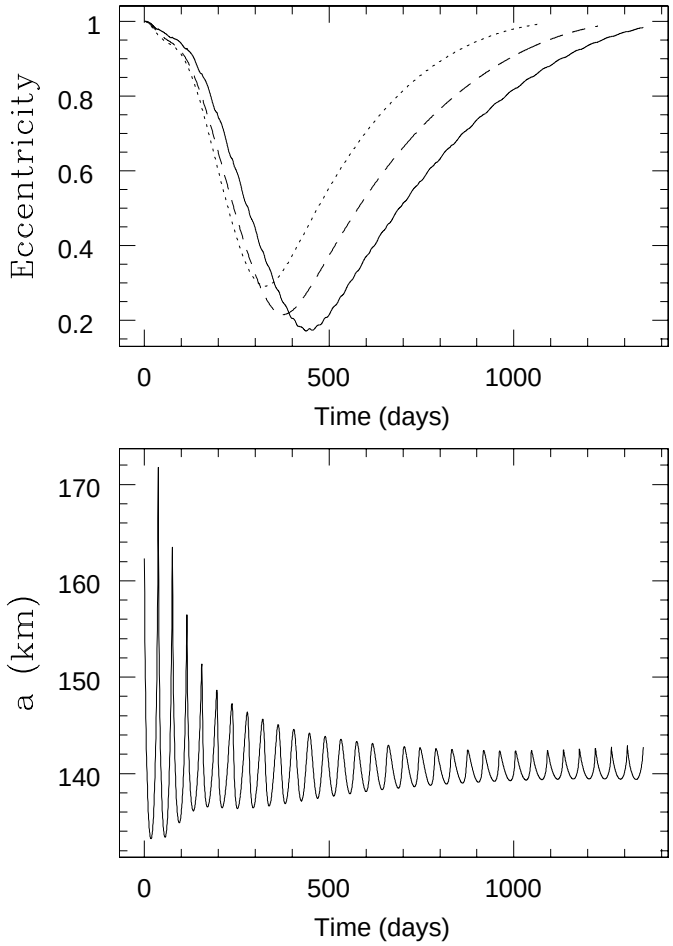

Fig. 3. Comparison between RPA (dotted line) and numerical integration (continuous line) for a large dust grain 5 cm in diameter. The large oscillations induced by solar tide cause the RPA prediction with average semimajor axis a = 170 km to depart from the numerical solution after 500 days. A better match to the numerical solution is obtained by assuming an 'effective' semimajor axis of 142 km in the RPA solution (dashed line).

In Fig. 2 we show the comparison between the RPA predictions (dotted line) and the numerical integration (continuous line) for a 1 cm dust particle. The eccentricity evolution predicted by the numerical simulation is well reproduced by RPA and the semimajor axis of the orbit is on average constant (as assumed in RPA) with small variations around the mean. Since the DI experiment occurs at the comet perihelium, the radiation pressure is relatively strong and even large particles in the cm-size range are affected. The dynamical evolution of a 5 cm dust particle is shown in Fig. 3: the difference between the evolution of the eccentricity computed numerically and calculated from RPA is mainly due to the oscillations in the semimajor axis of the orbit and by the solar tide. We can partly obviate this problem by modifing the RPA solution, introducing a mean semimajor axis computed from the numerical simulation. This is equivalent to modifying the modulus of the initial ejection velocity. As an example, in Fig. 3 we include the RPA solution (dashed line) where an averaged semimajor axis is used instead of that derived from the initial conditions of the numerical simulation. A better match between the analytical approximation and the numerical solution is obtained in this case.

If the difference between RPA and numerical simulation is always related to a change in semimajor axis due to the solar tide, then RPA still represents a good approximation on average. The solar tide will systematically modify the RPA predictions by shifting, for a given particle size and ejection site, the range of ejection velocities leading to temporary capture. This is shown in Fig. 4, the dashed line represents the RPA solution and the continuous line the numerical simulation. Above the upper curve, the particles hyperbolically escape while below the bottom curve the particles re-impact on the surface of the comet before completing one single orbit.

There are a few pathological exceptions to this picture. For particular initial conditions, the eccentricity evolves with a small initial bump, as shown in Fig. 5. The numerical integration shows that the eccentricity initially decreases but then rises back to high values on a short timescale. After this initial bump,

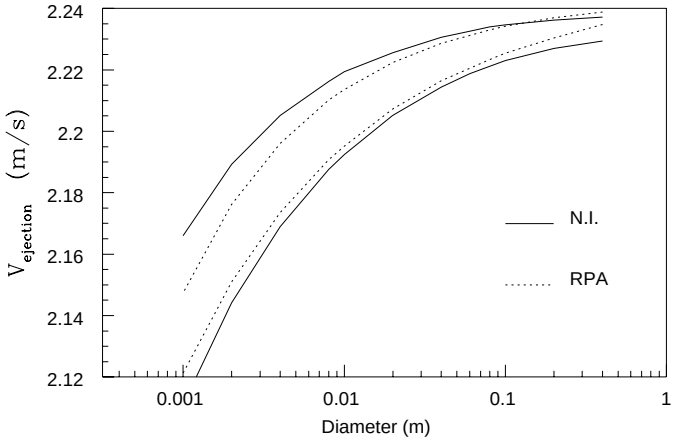

Fig. 4. Range of ejection velocities for different particle sizes leading to temporary capture around the comet. The dotted line is computed with RPA while the continuous line is the numerical solution.

the eccentricity slowly decreases to low values completing the cycle. RPA instead predicts that the particle will re–impact at the end of the short bump, since the eccentricity gets back to the initial high values and the pericenter falls inside the comet's radius. The difference between RPA and the numerical solution is still due to the solar tide. Fig. 5 shows that the numerical solution follows the evolution in eccentricity predicted by RPA at the beginning, but when the re–impact should occur, the semimajor axis has increased by the effect of the solar tide. The pericenter of the orbit remains larger than the comet radius and the temporary trapping lasts much longer since the grain completes an eccentricity cycle. The predictions of RPA in these cases are still reliable with regard to the interval of ejection velocities leading to temporary capture (Fig. 6). However, the lifetime estimates can be wrong by one order of magnitude. In Fig. 7 we compare the lifetime for a 5 cm particle emitted at different values of β. We see that the region where the RPA and numerical predictions do not agree for the pathological behaviour described above, are limited. The effects of the solar tide can also be noted in Fig. 7: the lifetime as a function of β from the numerical integration oscillates around the value predicted by RPA due to the change in the orbital energy. Depending on the orientation of the ejected particle (angle β) the solar tide changes its effect.

3.2. Solar tide

As noted above, the solar tide has an effect on the dynamics of ejected particles. We have included the major effect of this force by incorporating Eq. 7 into our analysis, which gives the upper limit on an ejected particle's semi-major axis before it is stripped from the comet.

As noted above there is also a systematic effect of solar tide. Based on results in the existing spacecraft dynamics literature (Yamakawa et al. 1993) we can show that the particles ejected in the first and third quadrants of longitude (between angles 0 and 90° or 180° and 270°) will have a decrease in orbit energy and angular momentum, while particles ejected in the second

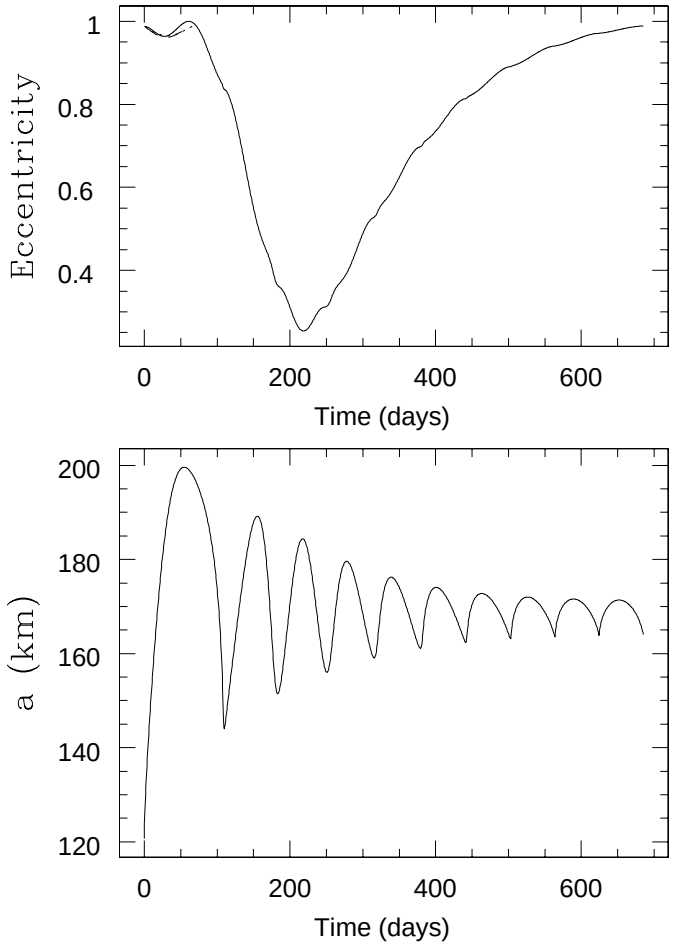

Fig. 5. Pathological case: RPA predicts a lifetime for trapping much smaller than that derived from the numerical simulation. The large oscillation in a in the first 100 days prevents the dust particle to re–impact on the comet at $t \sim 80$ days from the ejection, when the eccentricity grows close to 1. RPA fails to reproduce this behaviour since it assumes a constant a. According to RPA the particle re–impacts at $t \sim 80$ days.

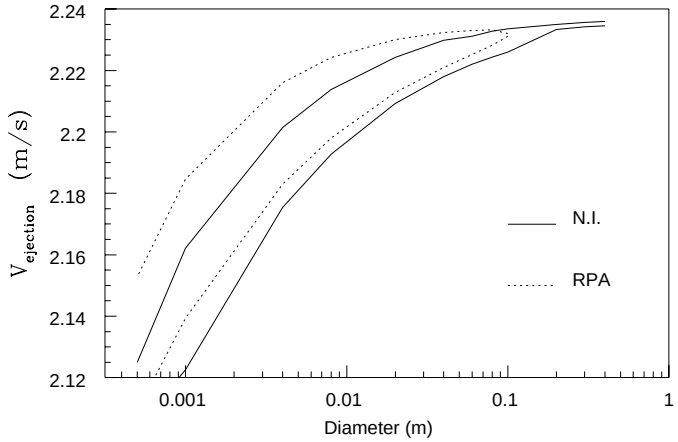

Fig. 6. In spite of the pathological behaviour described in Fig. 5, RPA predictions (dotted line) of the velocity ranges for trapping are in good agreement with the numerical ones (continuous line).

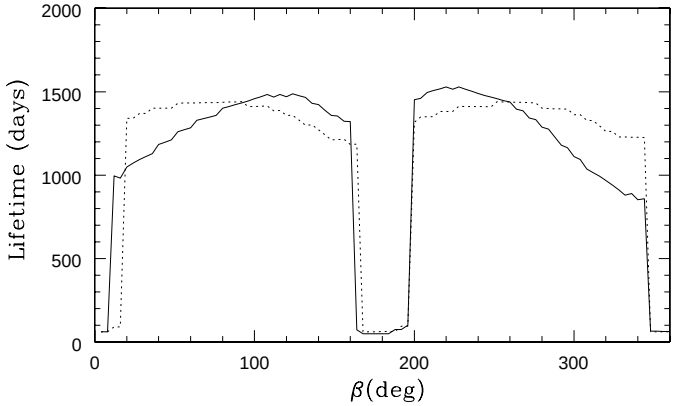

Fig. 7. Lifetimes computed with numerical integration (continuous line) and with RPA (dotted line) as a function of the ejection angle β for a 5 cm particle. The main differences between numerical and analytical solution are related to the effects of the solar tide.

and fourth quadrant of longitude (between angles 90 and 180° or 270° and 360°) will suffer a slight increase in orbit energy and angular momentum due to the solar tide interaction. Thus, for a given ejection site this will systematically shift the capture conditions of a set of particles. This does not play too large a role for statistical studies as we have here, as this is just a uniform shift in the ejection velocity that leads to capture. Future studies that look at capture conditions over the entire surface should take this effect into account, however.

3.3. Gravity field perturbations

Whenever an ejected particle has a close passage to the comet (generally within 5 - 10 mean radii) there is the potential for the comet gravity field to alter the particle orbit – resulting in either an increase or decrease in the orbit energy and angular momentum, depending on the precise conditions at closest approach. The effect of these interactions have been studied previously (Scheeres et al. 1996, 1998; Scheeres 1999) – the results of those analyses being applied here. Tempel 1 may have a fairly elongated shape, which corresponds to a large C_{22} gravity term and hence a greater efficiency in altering a particle orbit. It also has an assumed slow rotation period of 24 hours. This combination actually increases the effect of the comet nucleus gravity field on nearby orbits – meaning that the interaction may be important out to distances of $\sim$ 20 km. While the net effect of these interactions will average out over long time spans (i.e., over many close approaches), over finite numbers of interactions we often see strong transient changes in orbit energy and angular momentum. The short term effect of these interactions can be to either cause the particle to escape from the comet or cause the orbit to become more closely bound to the nucleus. The latter effect would also serve to effectively decrease the SRP strength parameter and hence diminish the effect of SRP on the orbit evolution. This would, in general, cause the orbit lifetime to increase significantly – barring any premature escape due to interactions with the gravity field.

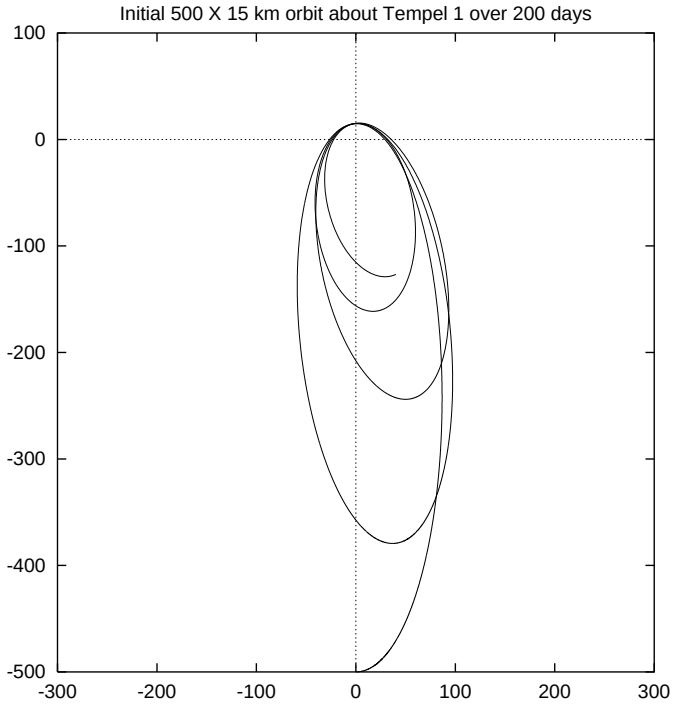

Fig. 8. Inertial trajectory of a particle orbit about Tempel 1 over 200 days. The initial orbit had an apoapsis radius of 500 km and a periapsis radius of 15 km.

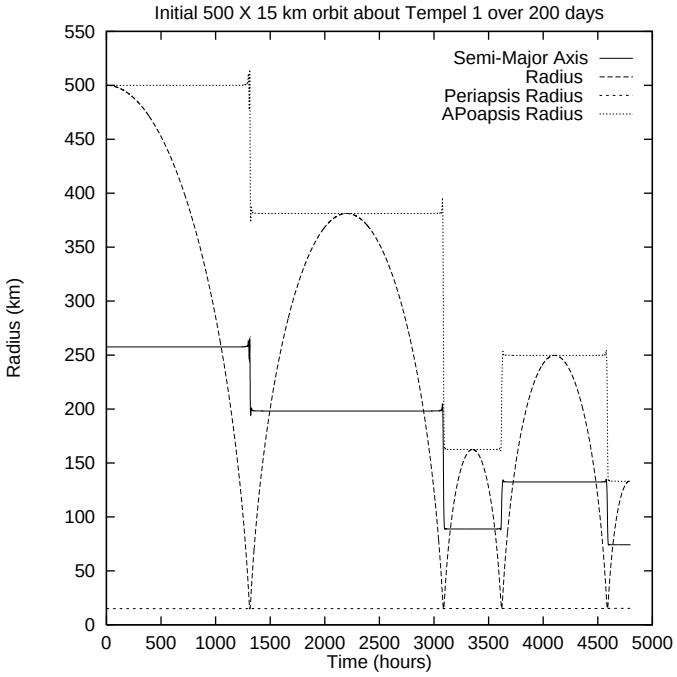

Fig. 9. Plots of the orbit radius, semi-major axis, apoapsis radius and periapsis radius over 200 days.

An explicit example of this type of behaviour is shown in Figs. 8 and 9 which show a trajectory about Tempel 1 over 200 days, with all changes in the orbit being due only to interactions with a rotating non-spherical Tempel 1 shape. In this compu-

tation we modeled Tempel 1 as an ellipsoid with half-axes of $4.76 \times 2.38 \times 2.38$ – a 2:1:1 shape ratio with a mean radius of 3 km. We gave the ellipsoid a constant density of 1 g/cm^3 and a 24 hour period uniform rotation about its maximum moment of inertia. The initial orbit has apoapsis at 500 km and periapsis at 15 km – mimicing a possible initial condition of a particle after SRP has raised its periapsis above the comet surface. We see that even at this distance – 5 mean radii away – the comet gravity field can have a significant effect on the particle orbit and will be an important effect to include in future, detailed analysis of crater ejecta dynamics.

3.4. Comet outgassing

The net effect of comet outgassing on a particle orbit is an issue currently under study. To properly model this effect requires the specification of a comet outgassing field – an endeavor that requires significant modeling assumptions and has few significant data points or measurements – especially for the field close to a comet. Nonetheless, plausible models for the outgassing at a comet exist and have been used to study particle and spacecraft dynamics (Fulle 1997; Scheeres et al 1998; Fulle 1999).

One particularly simple model specification assumes that the outgassing pressure varies as $1/r^2$ from the comet, acts in the radial direction, and varies continuously with solar phase angle, leading to an effective drag of the form:

$$f \;=\; \frac{\mu_d}{r^2}\cos^2(\phi/2) \tag{16}$$

where μ_d is equivalent to the mass parameter and combines the particle's mass to area ratio and the outgassing pressure, and is a function of the comet-sun distance (dropping to zero at some distance from the sun and rising to its maximum at perihelion), and ϕ is the phase angle of the particle as measured from the sub-solar point. This particular force field can be averaged over one particle orbit and the resulting equations can be analyzed (Scheeres et al. 1998). One interesting note, discussed in Scheeres & Marzari (1998), is that the resulting equations can be integrated in terms of the mean anomaly of the particle orbit – yielding a solution for the eccentricity of the particle orbit under outgassing pressure. If we assume that the initial orbit is rectilinear then we find the solution:

$$e^2 \;=\; 1 - \frac{\mu_d}{2\mu}\sin\delta\cos\alpha M + \left(\frac{\mu_d}{4\mu}\right)^2 \cos^2\alpha M^2 \tag{17}$$

where in general $\mu_d \ll \mu$ for a larger particle. We see that the initial eccentricity is equal to 1, and that eventually, for mean anomaly M large enough, the eccentricity will become greater than 1 – indicating that such an outgassing field will eventually cause all particles to escape. An important consideration to note is that the eccentricity may initially decrease from unity as a function of its ejection site – allowing the comet outgassing to help capture the particle.

Competing models of comet outgassing have the gas emanating from isolated locations on the comet surface. For these models the outgassing pressure will be relatively large inside the jet, causing a particle that crosses its path to receive a strong, impulsive change to its orbit (Scheeres et al. 1998). However, the probability for such a crossing to occur will be fairly low in general, unless there exists some resonance between the particle motion and the inertial attitude of the comet.

4. Application to the Deep Impact experiment

4.1. Comet model

To simplify the discussion of this problem we use the Deep Impact nominal impact event as a test bench for our computations. This represents an extreme case, since the orbit of comet Tempel 1 is highly eccentric and the event occurs at comet perihelion. The basic measured and assumed parameters for comet Tempel 1 are given in Table 1.

4.2. Ejection conditions from the surface

To model the impact scenario on the comet surface we constrain a number of the initial conditions. First, we specify that the impact occurs when the comet is at perihelion. The nominal impact site is at a latitude of -22 degrees (measured from the comet orbital plane) and a longitude of 116 degrees (measured from the anti-sun direction). The ejected particles are assumed to have the same density as the comet, and to have a spherical shape.

We model the initial conditions of the ejected particles as elliptic orbits with sub-escape speeds. In general, all particles that initially have greater than escape speed will not return or orbit the comet (some exceptions to this could occur due to the interaction of the solar tide with the particle). If no additional perturbations act on these sub-escape orbits they will, of course, re-impact on the surface after one orbit period. We assume that the ejection occurs at an angle γ of 45° with respect to vertical, which is a standard result derived from impact experiments. Note that this ejection geometry assumes that the shape of the comet is spherical. A small comet like Tempel 1 may have a very irregular shape that may invalidate the spherical approximation, however, the range of choices for the ejection geometry is in this case so wide that it would be impossible to consider all the alternatives. Our simulations, on the other hand, are intended to give a general view of the problem. The specific computations can only be done when the shape of the body and its rotation state is known in detail.

4.3. Global computations for the Deep Impact cratering event

The advantage of having a working analytical theory for computing the dust particle evolution resides in the capability of fast computations and a better understanding of how the physical parameters of the problem influence the motion. We can easily calculate the time evolution of a large number of orbits and derive the global behaviour of the dust cloud lofted by an impact. This is particularly useful if we intend to explore in detail the 3–dimensional parameter space (ejection velocity, and

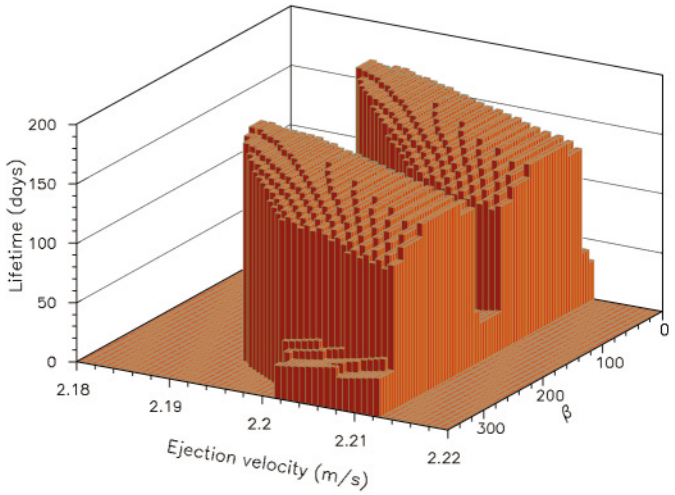

Fig. 10. Lifetimes of dust particles 1 cm in diameter for different values of the ejection velocity and ejection angle β.

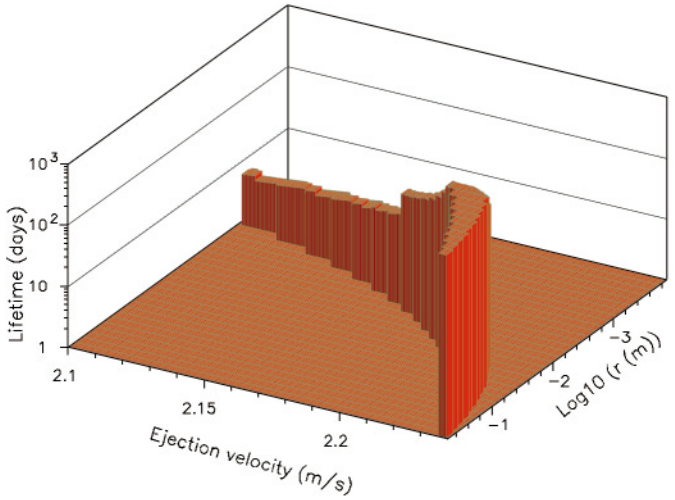

Fig. 11. Lifetimes of dust particles vs. size and ejection velocity. They are computed assuming a fixed value of β.

ejection angle β) that characterizes the orbits of dust particles ejected at a given impact site.

Fig. 10 is a 3–dimensional histogram where we plot the lifetimes of 1 cm particles as a function of their ejection speeds and ejection angle β. The sharp cut in the lifetimes for velocities larger than 2.21 m/s is related to the hyperbolic escape of faster particles. In Fig. 11 we plot the lifetimes as a function of size and ejection velocity. The 3–dimensional surface of Fig. 12 envelopes the capture regions in the v_e x β x r_p space. From the three figures we see that larger size grains have to be ejected at larger velocities to get captured in temporary orbits. As a consequence, after an impact large particles will, on average, have higher semimajor axes and, for most of the time, will orbit farther from the nucleus than smaller particles. The density of the dust cloud around the comet will have a gradient in the size of the grains, with smaller particles filling the zones close to the comet surface. From Fig. 11 we also notice that smaller

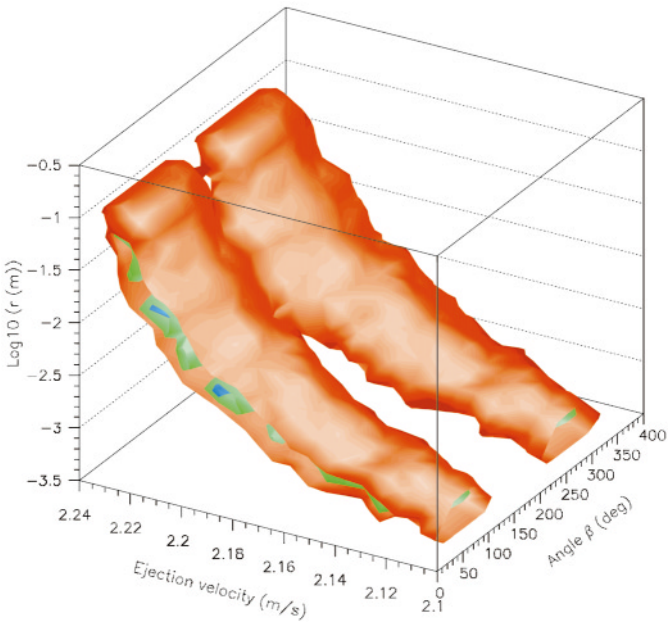

Fig. 12. Temporary trapping occurs within the surfaces shown in the: (ejection velocity in m/s) vs. β vs. (logarithm of size in m) space.

particles have short lifetimes as compared to the larger grains. The outer layers of the dust envelope that surrounds the nucleus after the impact will then survive longer and will be made of larger particles. From Fig. 12 we can also notice that all the ejection directions lead to trapping for larger grain sizes while smaller particles are trapped only if β is restricted around $100°$ and $300°$.

These useful statistical results are obtained running a simple numerical code based on RPA that gives the results in less than 5 min. of CPU time.

5. Conclusions

This paper shows that ejecta from cratering events can be placed into temporary orbits about asteroids or comets. The perturbations due to the solar radiation pressure can alter the initial orbital elements after the impact and transform re–impact orbits into a temporary capture orbits. By using an approximate analytical theory (RPA) we are able to explicitly compute the lifetime of particles as a function of their size, ejection site, ejection velocity, and ejection angles γ and β. We derive also the ranges of ejection velocity leading to capture instead of re–impact or hyperbolic escape.

We have performed numerical comparisons showing that the theory is qualitatively correct, making it useful for statistical studies at the least. Through this comparison we can also understand more precisely the physics behind temporary capture of particles about comets and asteroids. We used as a test bench the DI experiment at comet Tempel 1 and we found that dust grains from submillimeter to centimeters in size can be injected into temporary capture orbits around the comet after the experiment. We defined ranges in ejection velocity and ejection angles for trapping. These ranges are qualitatively correct and

are intended as useful indications to the more sophisticated numerical models that will be developed once the shape, gravity of the comet and outgassing activity of a particular comet are known.

There are a number of effects that are not accounted for in the RPA approximation, like irregularity of the gravity field, solar tide, and cometary outgassing. During our numerical study we could delineate how the predictions of RPA are affected by solar tide. However, we can only estimate the changes in the orbital evolution induced by the other two perturbing forces. Gravity field perturbations affect only a small percentage of particles whose periapses are very close to the nucleus during the temporary capture. If the pericenter passage occurs within 5 nucleus radii, the irregular field of the body can either eject the particle in a hyperbolic orbit or cause the particle to be more closely bound to the nucleus. Comet outgassing, if collimated into jets, represents a significant perturbation only if the particle crosses the jet. An extended outgassing field may alter the eccentricity of the orbit and again cause escape or even trapping.

Acknowledgements. The authors are very grateful for the comments of M. Fulle. DJS acknowledges support from NASA's Planetary Geology and Geophysics Program and by the TMOD Technology Program by a grant from the Jet Propulsion Laboratory, California Institute of Technology which is under contract with the National Aeronautics and Space Administration.

References

Everhart E., In: Carusi A., Valsecchi G.B. (eds.) Dynamics of Comets: Their Origin and Evolution, Proc. IAU Coll. 83, Dordrecht: Reidel, Astrophysics and Space Science Library, Vol. 115, 1985, p. 185

Fulle M., 1997, A&A 325, 1237

Fulle M., Crifo J.F., Rodionov A.V., 1999, A&A 347, 1009

Geissler P., Petit J.-M., Durda D., et al., 1996, Icarus 120, 140

Hamilton D.P., Burns J.A., 1992, Icarus 96, 43–64

Meech K.J., Bauer J.M., A'Hearn M.F., 1999, American Astronomical Society, DPS meeting 31, n. 30.02

Mignard F., Hénon M., 1984, Celestial Mechanics 33, 239

Richter K., Keller H.U., 1995, Icarus 114, 355

Scheeres D.J., Ostro S.J., Hudson R.S., Werner R.A., 1996 Icarus 121, 67

Scheeres D.J., Marzari F., Tomasella L., Vanzani V., 1998, Planet. and Space Sci. 46, 649

Scheeres D.J., Marzari F., 1998, Dynamics in the Cometary Environment. Poster presented at the 1998 AAS-DPS conference in Madison, WI, October 11-16

Scheeres D.J., 1999, Celestial Mechanics and Dynamical Astronomy 73, 339

Scheeres D.J., Marzari F., Spacecraft dynamics far from a comet. Submitted to the Journal of Astronautical Sciences

Yamakawa H., Kawaguchi J., Ishii K., Matsuo H., 1993, On Earth-Moon Transfer Trajectory with Gravitational Capture. Paper AAS 93-633, presented at the AAS/AIAA Astrodynamics Specialist Conference, Victoria, B.C., Canada, August 1993